Available online at www.sciencedirect.com
SCIENCE DIRECT
Journal of Controlled Release 111 (2006) 193–203
journal of controlled release
www.elsevier.com/locate/jconrel

Selective targeting of pentoxifylline to hepatic stellate cells using a novel platinum-based linker technology

Teresa Gonzalo [a,*], Eduard G. Talman [b], Anke van de Ven [a], Kai Temming [a,b], Rick Greupink [a], Leonie Beljaars [a], Catharina Reker-Smit [a], Dirk K.F. Meijer [a], Grietje Molema [c], Klaas Poelstra [a], Robbert J. Kok [a]

[a] *Department of Pharmacokinetics and Drug Delivery, Groningen University Institute for Drug Exploration, Antonius Deusinglaan 1, 9713 AV Groningen, The Netherlands*
[b] *Kreatech Biotechnology, Amsterdam, The Netherlands*
[c] *Department of Pathology and Laboratory Medicine, Medical Biology Section, Groningen University Institute for Drug Exploration, The Netherlands*

Received 22 July 2005; accepted 8 December 2005

Abstract

Targeting of antifibrotic drugs to hepatic stellate cells (HSC) is a promising strategy to block fibrotic processes leading to liver cirrhosis. For this purpose, we utilized the neo-glycoprotein mannose-6-phosphate-albumin (M6PHSA) that accumulates efficiently in HSC during liver fibrosis. Pentoxifylline (PTX), an antifibrotic compound that inhibits HSC proliferation and activation in vitro, was conjugated to M6PHSA. We employed a new type of platinum-based linker, which conjugates PTX via coordination chemistry rather than via covalent linkage. When incubated in plasma or in the presence of thiol compounds, free PTX was released from PTX–M6PHSA at a sustained slow rate.

PTX–M6PHSA displayed pharmacological activity in cultured HSC as evidenced by changes in cell morphology and reduction of collagen I production. PTX–M6PHSA and platinum coupled PTX did not induce platinum-related toxicity (Alamar Blue viability assay) or apoptosis (caspase activation and TUNEL staining). In vivo distribution studies in fibrotic rats demonstrated specific accumulation of the conjugate in nonparenchymal cells in the fibrotic liver. In conclusion, we have developed PTX–M6PHSA employing a novel type of platinum linker, which allows sustained delivery of the drug to HSC in the fibrotic liver.

Keywords: Drug targeting; Antifibrotic drugs; Linker technology; Liver fibrosis; Organoplatinum compounds

1. Introduction

Liver cirrhosis is the end-stage of liver diseases such as viral hepatitis, alcohol abuse, non-alcoholic steatohepatitis and other diseases in which acute liver damage leads to chronic inflammation and fibrosis [1]. Apart from liver transplantation, no appropriate treatment is currently available for liver fibrosis. Unfortunately, donor organ shortage and high costs remain a serious problem for transplantation and, when it occurs, hepatic failure after transplantation is still burdened by a high mortality rate. Finding a proper pharmacotherapeutic treatment for liver fibrosis is therefore considered a major challenge. Selective targeting of antifibrotic drugs to hepatic stellate cells (HSC) has recently been proposed as a potential new strategy to counteract liver fibrosis at the level of stellate cell activation [2]. HSC have been identified as the key fibrogenic cell type [3,4]. During liver fibrosis, different stimuli induce HSC proliferation, leading to large numbers of activated HSC that regulate the increased

Abbreviations: αSMA, α-smooth muscle actin; BCA, bicinchoninic acid; BDL, bile duct ligated; DMF, dimethylformamide; DTT, dithiothreitol; FAAS, flameless atomic absorption spectroscopy; FLU-ULS, adduct of fluorescein and platinum linker; GSH, glutathione; HSC, hepatic stellate cell; M6PHSA, mannose-6-phosphate modified human serum albumin; PTX, pentoxifylline; PTX-ULS, adduct of PTX en platinum linker; TUNEL, TdT-mediated dUTP Nick End Labeling; ULS, Platinum(ethylenediamine) linker, named Universal Linker System.

* Corresponding author. Tel.: +31 50 363 7567; fax: +31 50 363 3247.
E-mail address: T.Gonzalo.Lazaro@rug.nl (T. Gonzalo).

0168-3659/$ - see front matter © 2005 Elsevier B.V. All rights reserved.
doi:10.1016/j.jconrel.2005.12.010

production of extracellular matrix components such as collagens [5].

We have developed mannose-6-phosphate modified albumin (M6PHSA), which binds with high affinity to the insulin-like growth factor II/mannose-6-phosphate receptor on activated HSC [2,6,7]. Since the M6PHSA carrier is internalized via receptor-mediated-endocytosis upon binding to HSC, potent antifibrotic compounds can be delivered intracellularly within the diseased liver, and even within the desired cell-type [8].

Pentoxifylline (PTX) has been suggested for specific targeting to the fibrotic liver [1]. Its antifibrogenic and anti-inflammatory properties on activated HSC have been extensively reported and demonstrated. PTX reduces the transdifferentiation of HSC to myofibroblasts and inhibits HSC proliferation [9–11]. PTX also reduces the fibrogenic effect of TGF-β on HSC by interference with p38 MAP kinase and ERK1/2 pathways, thereby decreasing hepatic procollagen type 1 mRNA expression [12]. However, apart from beneficial effects in HSC, profibrotic effects of PTX on Kupffer cells have been reported [11], as well as many effects in other cell types [13,14]. Cell-selective targeting of PTX to HSC is therefore required to create favorable effects in HSC, while avoiding the profibrotic effects in Kupffer cells and effects in other organs.

In the present paper we describe the development of the novel HSC-directed conjugate PTX–M6PHSA. To conjugate PTX to M6PHSA, we employed a novel type of platinum linker chemistry which allows stable coupling of drug molecules to proteins. The new drug-linking approach is based on the formation of a platinum–ligand coordination bond with an aromatic nitrogen in PTX, after which the linker is further reacted to electron donor sites in the carrier protein (Fig. 1).

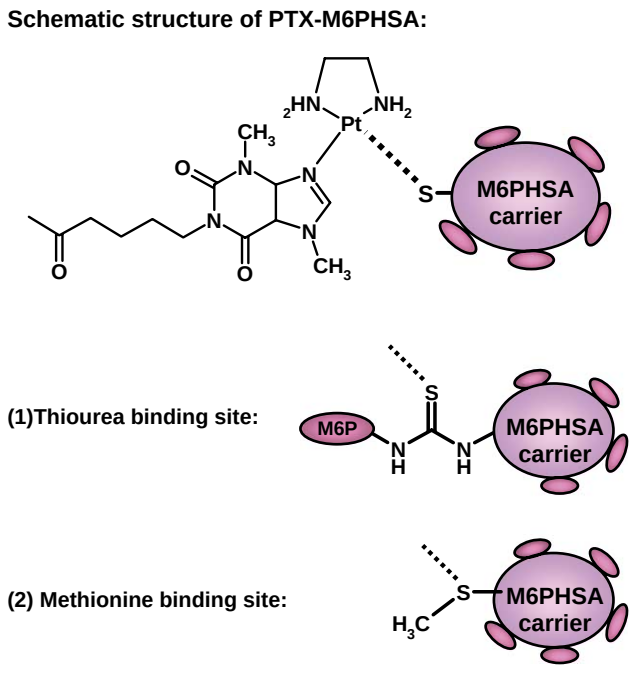

Fig. 1. General structure of PTX–M6PHSA. PTX is coupled via the platinum linker ULS to thiol groups of the protein. Two possible binding sites in the protein are proposed, i.e. the thiol group of the M6P homing devices on the modified HSA (1), and the sulfur atom in methionine groups of the protein (2).

Since the nature of the organoplatinum bond is quite different from the linkages in classical drug targeting conjugates, we investigated drug-release characteristics and linker-related toxicity of the conjugates. In addition, we report on cell-specific binding to HSC and in vitro pharmacological effects of PTX–M6PHSA, as well as its homing to HSC during liver fibrosis in the rat.

2. Materials and methods

2.1. Chemicals and biochemicals

Platinum (II) ethylendiammine dichloride (Universal linker System, ULS) and fluorescein-ULS (FLU-ULS) were prepared as previously described by Kreatech Biotechnology (Amsterdam, The Netherlands) [15]. PTX and cisplatin were obtained from Sigma. Human Serum Albumin (HSA) was obtained from Sanquin (Amsterdam, The Netherlands).

2.2. Synthesis of conjugates

2.2.1. Preparation of M6PHSA

M6PHSA was prepared and characterized as described previously [6]. Dimeric protein products which often are present in starting material or formed during reactions were removed by size-exclusion chromatography using a Hiload 16/60 Superdex 200 column (Amersham Biosciences). The final monomeric product was extensively dialyzed against water at 4 °C, lyophilized and stored at −20 °C until use. Typically, M6PHSA contains 28 M6P groups per albumin.

2.2.2. Synthesis of PTX-ULS

ULS (82.5 mg, 0.25 mmol) was dissolved in 3 ml of dimethylformamide (DMF) and converted into the more reactive ULS mononitrate by adding small aliquots of $AgNO_3$ (38.5 mg, 0.22 mmol, dissolved in 1 ml of DMF) within a time period of two hours. The precipitated AgCl was removed by centrifugation. PTX (43.2 mg, 0.155 mmol, dissolved in 1 ml of DMF) was added and the resulting mixture was stirred at 60 °C for 2 days. DMF was removed by rotary evaporation, after which the residue was dissolved in 2 ml of water and again taken to dryness under reduced pressure. The crude product was dissolved in water (2 ml) and stored overnight at −20 °C to precipitate unreacted ULS as yellow crystals, which were removed by centrifugation (10 min at 14,000 rpm). The identity and purity of the final product were checked by HPLC (95%), NMR and mass spectroscopy. PTX-ULS was stored at 4 °C until further use.

Yield: 105 mg (0.166 mmol, 107% yield). Apart from PTX-ULS, the product contained water and inorganic salts that did not interfere in the next reaction step.

PTX ^{1}H NMR (D_2O): δ_H 1.61 (m, 4H, $CH_2(CH_2)_2CH_2$), 2.24 (s, 3H, CH_3CO), 2.64 (t, J=6.41 Hz, 2H, $COCH_2$), 3.53 (s, 3H, $CONCH_3$), 3.95 (m, 5H, CH_2N and $CNCH_3CH$), 7.92 (s, 1H, CH) ppm.

PTX-ULS ^{1}H NMR (D_2O): δ_H 1.62 (m, 4H, $CH_2(CH_2)_2CH_2$), 2.25 (s, 3H, CH_3CO), 2.58 (m, 6H, $COCH_2$,

H2N(C**H₂)₂**NH₂), 3.99 (t, *J*=6.56 Hz, 2H, C**H₂**N), 4.02 (s, 3H, CONC**H₃**), 4.55 (s, 3H, CNC**H₃**C), 5.59 (m, 4H, **H₂**N(CH₂)₂N**H₂**), 8.48 (s, 1H, C**H**) ppm.

PTX-ULS ^{195}Pt NMR (D_2O): δPt −2471 ppm.

PTX-ULS ionspray MS: Observed product peaks corresponded to PTX-ULS monochloride (MW=568.1 Da) and to PTX-ULS in which chloride was replaced by a hydroxyl anion (MW=550.1 Da). The latter product is possibly formed during dilution or ionization of the compound for mass analysis. Both PTX-ULS species will react similarly in subsequent reaction steps.

2.2.3. Synthesis of PTX–M6PHSA and other conjugates

All PTX-ULS–protein and FLU-ULS–protein conjugates listed in Table 1 were prepared according to the following general protocol, which employs a 10:1 molar ratio of drug-ULS to protein. Typically, 10 mg of M6PHSA (143 nmol) was dissolved in 1 ml of 20 mM tricine/$NaNO_3$ buffer pH 8.3. PTX-ULS (1430 nmol, 28.6 μl from a 50 mM stock solution in water) was added and the pH was checked and corrected if necessary. The mixture was reacted overnight at 37 °C, after which unreacted PTX-ULS was removed by size-exclusion chromatography using disposable PD10 columns (Amersham Biosciences), or by dialysis against PBS at 4 °C. The final product was sterilized by 0.2 μm filtration and stored at −20 °C.

2.3. Characterization of drug–protein conjugates

To determine the amount of PTX or FLU conjugated via ULS to the proteins, products were subjected to various analyses related to either carrier, drug or linker, respectively.

2.3.1. Protein determination

The protein content of the conjugates was analyzed by different standard protein assays. Both Lowry and Bradford assays yielded protein recoveries over 100%, indicating interference of ULS modification with the protein determination. The bicinchoninic acid (BCA) assay (Pierce, Rockford, IL, USA) resulted in adequate recovery of freeze-dried amounts of the products.

2.3.2. PTX determination

The amount of PTX coupled to the carrier was analyzed by HPLC after competitive displacement of the drug by excess of potassium thiocyanate (KSCN), a Pt-coordinating ligand. In brief, appropriate dilutions of the conjugates corresponding to approximately 10 μM PTX were incubated overnight at 80 °C in the presence of 0.5 M KSCN in PBS. After cooling to room temperature, the samples were stored at −20 °C until HPLC analysis. Free, non-conjugated PTX was determined by HPLC analysis of samples that had not been incubated with KSCN.

We analyzed PTX and PTX-ULS by reverse-phase HPLC on a Waters system (Waters, Milford, MA, USA) equipped with an UV detector operated at 274 nm and a thermostated column oven operated at 40 °C. Elutions were performed on a μBondapak Guard-pak C18 precolumn in combination with a 5 μm Hypersil BDS C8 column (250×4.6 mm, Thermoquest Runcorn, UK). Mobile phase consisted of acetonitrile/water/trifluoracetic acid (25/75/0.1) at 1 ml/min. PTX and PTX-ULS eluted at 6 and 5 min after injection, respectively.

Table 1
Characterization of conjugates synthesized with PTX-ULS and FLU-ULS

Conjugate	Synthesis ratio drug-ULS:protein	Coupling ratio drug:protein [a]	Coupling ratio ULS:protein [b]
PTX–M6PHSA	10:1	6.7:1 (±0.7)	6.9:1 (±2.7)
PTX-HSA	10:1	1.5:1 (±1.0)	3.5:1 (±2.1)
FLU-M6PHSA	10:1	6.5:1 (±2.0)	6.2:1 (±2.9)
FLU-HSA	10:1	4.3:1 (±2.0)	5.4:1 (±0.4)

[a] PTX coupling ratio was determined by HPLC after competitive displacement of the drug with KSCN at 80 °C for 24 h. FLU coupling ratio was determined by its absorbance at 500 nm.

[b] ULS coupling ratio was determined by FAAS.

2.3.3. Characterization of FLU-ULS modified proteins

FLU-ULS coupling ratios were determined spectrophotometrically without destruction of the conjugates. Appropriate dilutions of the conjugates in PBS were analyzed at 500 nm and related to a calibration curve of fluorescein sodium.

2.3.4. Determination of platinum content in conjugates

To assess the number of coupled ULS molecules, appropriate dilutions of the conjugates corresponding to approximately 1 μM of platinum were analyzed by flameless atomic absorption spectroscopy (FAAS), as described previously [16].

2.4. PTX release studies

The stability of PTX–M6PHSA in biological media was investigated by incubating the conjugate in pH 7.4 at 37 °C up to 7 days in a 1:1 dilution of normal rat serum and PBS. Released PTX and conjugate bound drug were separated by treating aliquots with acetonitrile (2:1 v/v) after which the samples were centrifuged at high speed to precipitate proteins. The clear supernatant was stored at −20 °C until HPLC analysis. Calibration curves were made by spiking biological media with free PTX and were treated similar to PTX–M6PHSA samples.

Thiol-competitive displacement, rather than enzymatic release, most likely facilitates intracellular release of PTX from the conjugates. We therefore performed drug release studies by incubating PTX–M6PHSA for 24 h at 37 °C in PBS pH 7.4 containing 5 mM glutathione (GSH) or 5 mM dithiothreitol (DTT). PTX release was compared to incubations in PBS or HSC culture medium, and expressed as the percentage of total bound PTX.

2.5. Isolation and culturing of HSC

HSC were isolated from livers of male Wistar rats (0.3 kg) according to standard techniques [17]. After digestion of the liver with collagenase P (Boehringer, Mannheim, Germany), pronase (Merck, Darmstadt, Germany), and DNAse (Boehringer),

HSC were separated from other hepatic cells by density-gradient centrifugation and collected at the top of an 11% Nycodenz-solution (Brunschwig Chemie, Amsterdam). Subsequently, HSC were cultured in disposable plastic bottles (Nunc, USA), in DMEM (GIBCO) containing 10% fetal calf serum (Hyclone Laboratories Inc., Logan, UT, USA), 100 U/ml penicillin, and 100 μg/ml streptomycin (Sigma). These culture conditions allow HSC to attach and proliferate as confirmed by microscopical evaluation. Cells cultured for 2 days after isolation exhibited the phenotype of quiescent HSC, a compact cell shape with many cytoplasmic fat droplets, while cells cultured for 10 days after isolation displayed the more elongated phenotype of activated HSC without the vitamin A containing fat droplets. All experiments with conjugates were performed with the latter type of activated HSC.

2.6. Binding studies of PTX–M6PHSA to target cells

2.6.1. M6P/IGFII receptor expression

We investigated the specific binding of PTX–M6PHSA to its target receptor in a cell line that express M6P/IGFII receptor. First, immunohistochemical detection of the target receptor was analyzed. For this purpose, NIH/3T3 cells (2500 cells/well seeded into 96 well-plates) were cultured for 24 h at 37 °C in DMEM medium (Cambrex, New Jersey) supplemented with 5% FCS. After washing and acetone-fixation of the cells, expression of the M6P/IGFII receptor was visualized by immunohistochemical staining (Santa Cruz Biotechnology, California).

2.6.2. Radioactive binding studies

In addition, we studied the binding of ^{125}I-radiolabeled PTX–M6PHSA to M6P/IGFII receptor expressing NIH/3T3 fibroblasts. PTX–M6PHSA was radiolabeled to a specific activity of 35×10^6 cpm/μg by a chloramine-T method. Prior to the experiment, the radiolabeled PTX–M6PHSA was purified by gel filtration on a PD10 column (Amersham Biosciences). After gel filtration, the radiolabeled PTX–M6PHSA contained less than 5% free ^{125}I, as determined by precipitation of the protein with 10% trichloroacetic acid.

Binding studies were performed by incubating NIH/3T3 cells (60,000 cells/well seeded in 12-well plates) with 100,000 cpm of radiolabeled PTX–M6PHSA for 4 h at 37 °C. Competitive displacement was performed by adding 0.1 mg/ml M6PHSA carrier. After washing of the cells with ice-cold PBS containing 1% bovine serum albumin, cells were lysed by adding 0.5 ml of 1 M NaOH for 30 min. ^{125}I-radioactivity was counted in an LKB multichannel counter (LKB, Bromma, Sweden).

2.6.3. Immunohistochemical binding studies

In addition we performed studies in which binding of PTX–M6PHSA was detected by immunohistochemical staining of the protein. For this purpose, NIH/3T3 cells were incubated for 4 h at 37 °C in the presence of 1 mg/ml M6PHSA or PTX–M6PHSA. After washing and acetone-fixation of the cells, the binding of the conjugates was detected immunohistochemically using rabbit-anti-HSA antibody (Cappel ICN Biomedicals, Zoetermeer, The Netherlands).

2.7. Binding/homing studies in BDL rats

Organ distribution studies were performed in BDL rats as described previously [2]. All in vivo experiments were approved by the Local Committee for Care and Use of Laboratory Animals. Male Wistar rats weighing 250–350 g (Harlan, Zeist, The Netherlands) were housed under a 12-h dark/light cycle. Animals had free access to tap water and standard lab chow. Liver fibrosis was induced by ligation of the bile duct under isoflurane anesthesia (2% isoflurane in 2 : 1 O_2/N_2O, 1 l/min) (Abbot Laboratories Ltd., Queensborough, UK). Three weeks after BDL, the liver showed severe fibrotic lesions and excessive matrix deposition, as assessed by immunostaining for collagen III [2]. At this time point, the rats were used for biodistribution studies to determine homing to the fibrotic liver and subcellular localization within the liver. During biodistribution studies, rats were kept under isoflurane anesthesia and body temperature was maintained at 37–38 °C.

2.7.1. Biodistribution of radiolabeled proteins

Rats were i.v. injected via the dorsal penis vein with tracer doses (10^6 cpm/rat) of either ^{125}I-PTX–M6PHSA or ^{125}I-radiolabeled M6PHSA. At 10 min after administration, blood samples were taken by heart puncture and the organs were excised, washed in saline, and weighed after which ^{125}I-radioactivity was counted. Urine was recovered from the bladder and measured. The total radioactivity per organ was calculated and corrected for blood-derived radioactivity using BDL correction factors.

2.7.2. Immunohistochemical detection of conjugates

In order to analyze intrahepatic distribution of the conjugates, BDL rats received one i.v. injection of non-radiolabeled PTX–M6PHSA (2 mg/kg). Tissue specimens were processed for immunohistochemical analysis according to standard procedures. Cryostat sections (4 μm) of the liver were fixed in acetone and stained for the presence of conjugates by anti-HSA immunodetection. Colocalization of PTX–M6PHSA with HSC was investigated by double staining of HSA and desmin. To amplify anti-HSA staining, GARPO (peroxidase-conjugated goat anti-rabbit immunoglobulin) and RAGPO (peroxidase-conjugated rabbit anti-goat immunoglobulin) secondary antibodies were used in the double staining protocol. Anti-desmin (Cappel ICN Biomedicals) was used in combination with RAM-AF (alkaline phosphatase-conjugated rabbit anti-mouse) for detection of activated HSC.

2.8. In vitro effects of PTX–M6PHSA conjugates

We tested the pharmacological efficacy of PTX–M6PHSA by incubating activated HSC for 24 h at 37 °C with the conjugate or with control compounds relating to the experiments described below.

2.8.1. Cytotoxic effects

Cell viability was determined using the Alamar Blue viability assay according to the protocol of the supplier (Serotec Ltd). Activated HSC (10,000 cells/well seeded in 96 well-plates, Corning Costar) were incubated for 24 h in culture medium spiked with either cisplatin (100 μM), PTX (100 μM), PTX-ULS (100 μM) or PTX–M6PHSA (1 mg/ml based in protein concentration, 100 μM in platinum concentration).

Induction of apoptosis was determined by caspase 3/7-activity measurement using the apoptosis Caspase-Glo assay (Promega). Activated HSC (10,000 cells/well seeded in white-walled 96 well-plates, Corning Costar) were incubated in culture medium spiked during 24 h with either cisplatin (100 μM), PTX (100 μM), PTX-ULS (100 μM) or PTX–M6PHSA (1 mg/ml based in protein concentration, 100 μM in platinum concentration).

Similar studies were performed with HSC (10,000 cells/well in Permanox LAB-TEK chamber slides, Nalge Nunc Int.) which were subjected to TUNEL staining of fragmented DNA as read-out parameter of apoptosis induction [18]. Quantification per treatment was performed after a minimum of 100 cells in at least 6 different microscopic fields per section at magnification of 10×, under the fluorescence microscope. Analysis performed by two independent observers.

2.8.2. Antifibrotic effects

HSC (10.000 cells/well in Permanox LAB-TEK chamber slides) were incubated with culture medium supplemented with either PTX–M6PHSA, PTX-HSA, or FLU-M6PHSA, all at a concentration of 1 mg/ml. The applied concentration of PTX–M6PHSA corresponded to 100 μM of conjugated PTX. In addition, HSC were incubated with 1 mM free PTX. After 24 h of incubation at 37 °C, HSC were acetone-fixed and stained for the presence of fibrosis markers according to standard methods using monoclonal antibody against α-smooth muscle actin (Sigma) or polyclonal antibody against collagen type I (Southern Biotechnology, USA). HSC morphology was analyzed via direct optical microscopy observation.

2.9. Statistics

Statistical significance of differences was tested using the two-tailed Student's *t*-test, assuming normal distribution and similar variances of the data. The differences were considered significant at *p*-values lower than 0.05. The data are presented as the mean of a triplicate ±S.D.

3. Results

3.1. Synthesis and characterization

In the present study, we investigated platinum-based coordination chemistry for the coupling PTX to the M6PHSA carrier protein. This new type of linker binds to aromatic nitrogens in drug molecules (Fig. 1), forming a bond of intermediate binding strength. To quantify PTX loading onto M6PHSA, the complexed drug was displaced by an excess of competing platinum–ligand (KSCN). The drug/carrier ratios as shown in Table 1 were corroborated by determination of platinum/carrier ratios using FAAS. Using a 10:1 initial synthesis ratio, an average of about 6 to 7 molecules of PTX-ULS was coupled to M6PHSA. Interestingly, coupling ratios of both PTX-ULS and FLU-ULS with M6PHSA exceeded those of conjugates prepared with unmodified HSA. Similarly, PTX-ULS showed also higher drug:carier loading ratio's with other neoglycoproteins like mannose-HSA (data not shown). Since platinum(II) readily reacts with sulfur containing ligands, we hypothesized that ULS reacted to the thiocarbonyl group between the M6P ligand and the albumin core protein, as illustrated in Fig. 1. Thiourea reacted rapidly with PTX-ULS at the applied reaction conditions of the conjugates, as was demonstrated by HPLC analysis and mass spectrometry (data not shown). However, reaction of ULS to other functional groups in the protein like methionine or cysteine residues or even hydroxyl or amine side chains cannot be excluded.

3.2. Drug release profile of PTX–M6PHSA conjugate

To study the stability of PTX–M6PHSA under physiological conditions, we incubated PTX–M6PHSA in serum (pH 7.4) at 37 °C. About 40% of the conjugated PTX was still bound to the

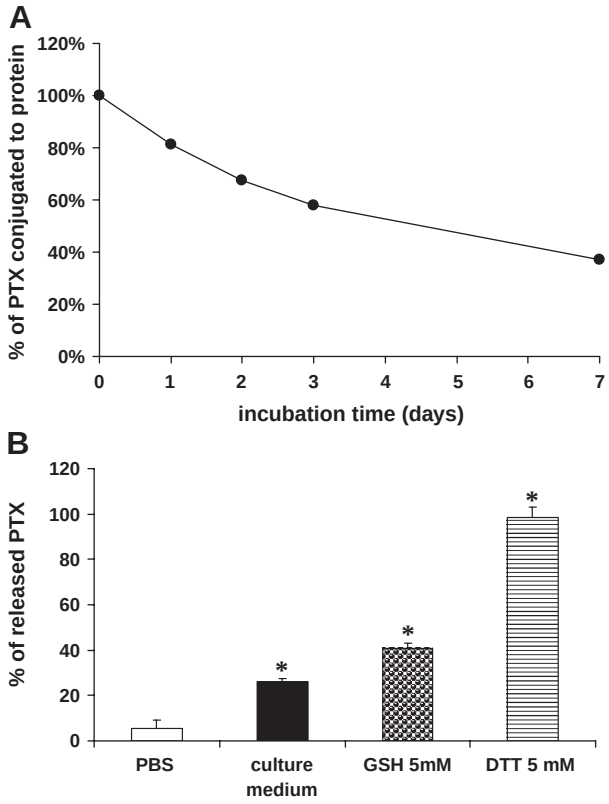

Fig. 2. Drug release profiles of PTX–M6PHSA. Released drug was related to the total amount of coupled PTX as determined by KSCN displacement. A) Drug release upon incubation of PTX–M6PHSA in serum/PBS (1:1) pH 7.4 at 37 °C for 7 days, B) Release of PTX after 24 h of incubation at 37 °C in PBS pH 7.4, HSC culture medium, or in the presence of thiol-containing competitors (GSH and DTT). *: $p<0.05$ vs PBS.

carrier after 7 days of incubation (Fig. 2A). This result indicates that the linkage between drug and carrier displays adequate stability in plasma, although the drug is released at a slow rate. PTX-HSA showed similar stability as PTX–M6PHSA (data not shown).

Since the release of PTX from the platinum is most likely due to competitive displacement by preferred platinum ligands, such as for instance thiols, we incubated the conjugate with DTT or GSH. Incubation with the non-physiological molecule DTT resulted in complete release of the drug from the conjugate (Fig. 2B). The concentration of 5 mM GSH reflects conditions within a cell's interior. GSH clearly accelerated the release of PTX from the carrier, as compared to incubation of the conjugate in PBS or culture medium. This result indicates that free PTX can be generated from the conjugate inside target cells.

We also incubated PTX–M6PHSA in different buffers at either cytosolic pH (PBS 7.4) or lysosomal pH (0.1 M sodium acetate buffer, pH 5.0). No differences were observed between pH 5 and 7 (data not shown). This result indicates that the drug release profile will not be affected by lysosomal pH.

3.3. Binding of PTX–M6PHSA to target cells

Since our characterization reactions revealed that ULS reacted to the thiourea-part of the M6P groups, binding properties of M6PHSA to M6P/IGFII receptor might be perturbed after coupling of PTX-ULS. After establishing the presence of our target receptor in a NIH/3T3 fibroblast cell line (Fig. 3A), we investigated binding of PTX–M6PHSA to these target cells. The observed binding of ^{125}I-PTX–M6PHSA to the cells could be displaced by competition with excess of M6PHSA (Fig. 3B). We therefore concluded that PTX–M6PHSA bound specifically to the cells via to M6P/IGFII receptor. In addition, non-radiolabeled PTX–M6PHSA was incubated with 3T3 fibroblasts, after which we visualized binding of PTX–M6PHSA to the cell surface by anti-HSA

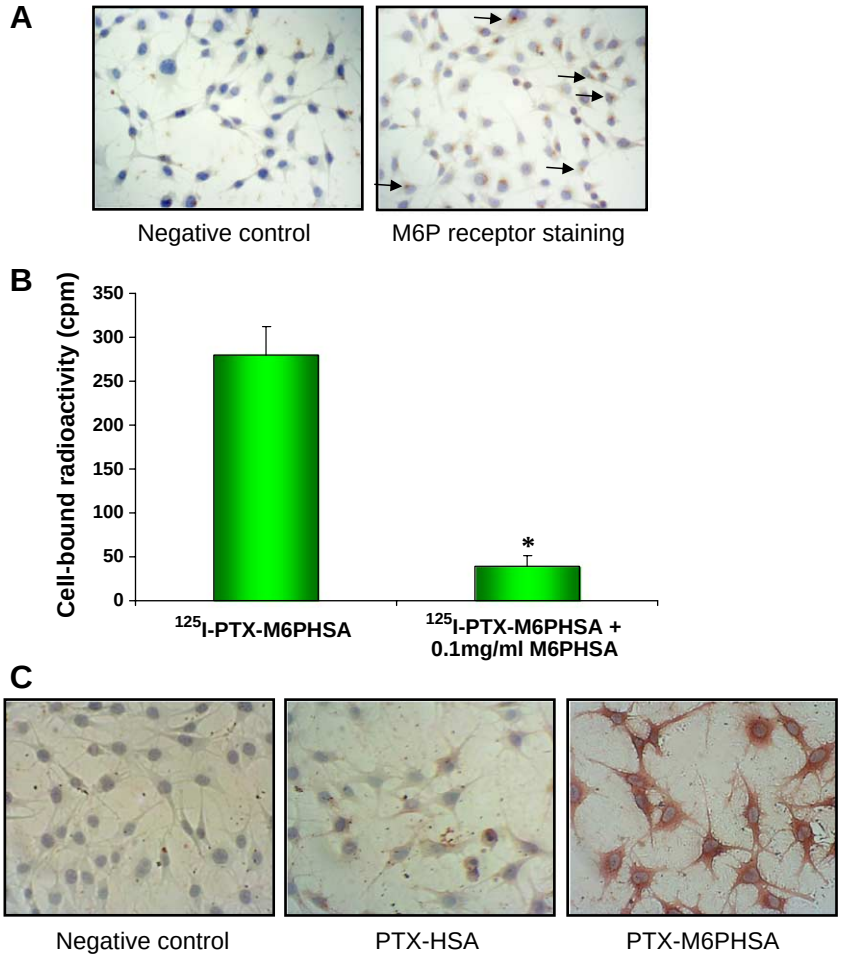

Fig. 3. PTX–M6PHSA binding to target cells. A) M6P/IGFII Receptor expressing NIH/3T3 fibroblasts were subjected to anti-M6P Receptor staining (red color) and hematoxillin counterstained (blue color). Note the receptor presence next to cell nuclei. Magnification 20×. B) NIH/3T3 cells were incubated with a tracer dose of ^{125}I-PTX–M6PHSA (100.000 cpm/well) in the absence or presence of excess M6PHSA (0.1 mg/ml) which were incubated for 4 h at 37 °C. *: $p<0.05$. C) NIH/3T3 fibroblasts were incubated with PTX-HSA or PTX–M6PHSA at 1 mg/ml for 4 h at 37 °C, after which the cells were stained for bound products using anti-HSA antibody (red color) and hematoxillin counterstained (blue color). Magnification 20×.

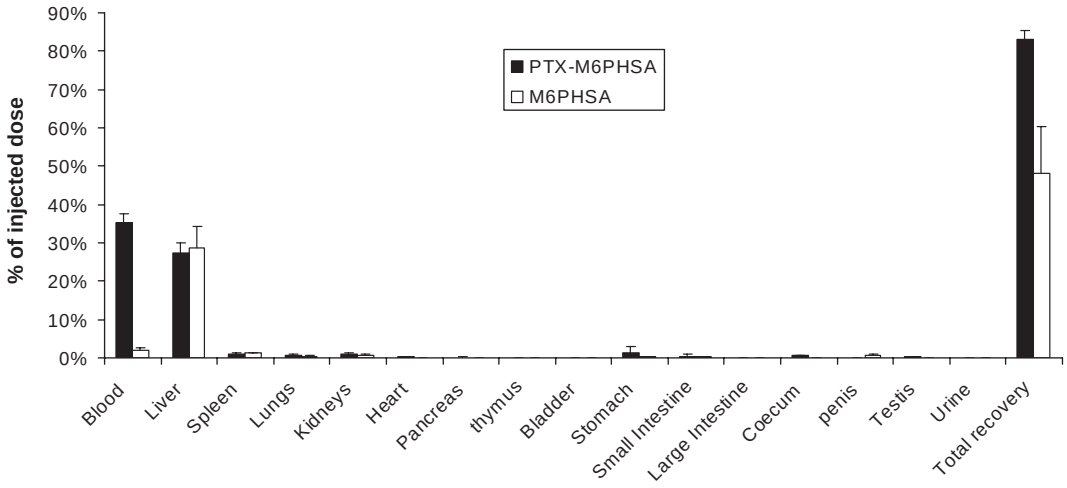

Fig. 4. Organ distribution of ^{125}I-PTX–M6PHSA and ^{125}I-M6PHSA in BDL rats. Tissue distribution of radiolabeled proteins was determined 10 min after intravenous injection of a tracer dose (1,000,000 cpm) of the radiolabeled proteins. Total radioactivity in the organs was corrected for blood-associated radioactivity and expressed as % of the injected dose. White bars: ^{125}I-M6PHSA, and black bars: ^{125}I-PTX–M6PHSA.

immunodetection (Fig. 3C). While PTX–M6PHSA showed intense positive staining, PTX-HSA did not bind to the cells. Thus, binding of PTX–M6PHSA to target cells was mediated via the M6P homing ligands in the conjugates.

3.4. Biodistribution of PTX–M6PHSA in rats with liver fibrosis

In addition to experiments with in vitro cultured target cells, we studied the biodistribution of PTX–M6PHSA in rats with liver fibrosis. Previous studies in our group have demonstrated that M6PHSA accumulates rapidly and efficiently in HSC within the fibrotic livers of BDL rats [2]. The initial distribution of M6PHSA could be assessed at ten minutes after injection. In the current experiment, we observed a rapid distribution of ^{125}I-radiolabeled PTX–M6PHSA and ^{125}I-radiolabeled M6PHSA to the fibrotic liver (Fig. 4). No accumulation in other organs was observed.

Within the fibrotic liver, PTX–M6PHSA displayed an HSC-like distribution pattern, as demonstrated by colocalization of carrier and desmin (Fig. 5). From these results we concluded that PTX–M6PHSA quickly distributed to the liver of BDL rats, where it specifically binds to HSC.

3.5. In vitro pharmacology of PTX–M6PHSA and control compounds

The pharmacological effects of PTX–M6PHSA conjugates were evaluated on activated HSC. Since cisplatin is a well-known antitumor agent, the use of platinum(II) as a linker may infer platinum-related toxicity into the drug targeting construct. We therefore investigated the effects of the conjugates on cell viability and apoptosis. Cell viability studies did not show any toxicity to the target cells after 24 h treatment with PTX, PTX-ULS or PTX–M6PHSA, in contrast to cisplatin at the same concentration (Fig. 6A). Similarly, treatment of HSC with cisplatin for 24 h induced apoptosis, as reflected in activation of caspases 3 and 7 (Fig. 6B), and the occurrence of DNA strand breaks assessed by TUNEL staining (Fig. 6C). Again, PTX, PTX-ULS and PTX–M6PHSA did not induce direct activation of caspases or apoptosis (Fig. 6B). Quantification of the

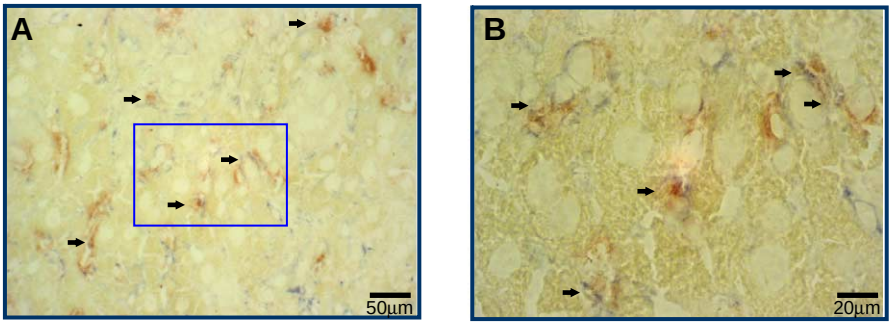

Fig. 5. Colocalization of PTX–M6PHSA with HSC in fibrotic livers of BDL rats. Animals were intravenously injected with 2 mg/kg of PTX–M6PHSA and sacrificed 10 min after administration. Picture A: Double staining for HSA (red) and the HSC marker desmin (blue). Arrows indicate colocalization of HSA and HSC. Magnification 40×. Picture B: Enlargement of picture A (100×).

TUNEL positive nuclei versus DAPI stained nuclei of HSC showed a significant increase after incubation with cisplatin, but no increase when cells were incubated with PTX–M6PHSA (Fig. 6D).

One of the hallmarks of liver fibrosis is the induced production of α-smooth muscle actin (αSMA) and collagen type 1 by activated HSC. We therefore investigated the expression of these proteins as read-out parameters for antifibrotic effects of PTX. As can be seen in Fig. 7, activated HSC express collagen type I in a granular staining pattern in the cytoplasm, probably reflecting the presence of procollagen type I, while αSMA stained in a fiber-like pattern. Treatment with PTX in a concentration of 1 mM reduced the intensity of both fibrotic markers (Fig. 7G,H). Incubation of the cells for 24 h with 1 mg/ml PTX–M6PHSA, which corresponds to 100 μM conjugated PTX, affected collagen type I expression considerably (Fig. 7E). Although the αSMA-staining intensity was not affected by PTX–M6PHSA, pronounced changes in the morphology of HSC were observed (Fig. 7F). HSC reacted to the treatment of PTX–M6PHSA with a loss of cytoplasmic volume, rounded cell shape and detachment of the cells from the surface of the plates. These effects were not observed after incubation with equivalent concentrations of PTX-HSA (Fig. 7C,D) or FLU-M6PHSA (data not shown), indicating that the targeted drug induced these effects.

4. Discussion

In the present paper, we report on a novel drug targeting preparation for the delivery of the antifibrotic drug PTX to HSC. Considering the important role of HSC in liver fibrosis, intervening with stellate cell activation seems an attractive approach to counteract liver fibrosis. We demonstrated accumulation of PTX–M6PHSA in HSC and observed promising in

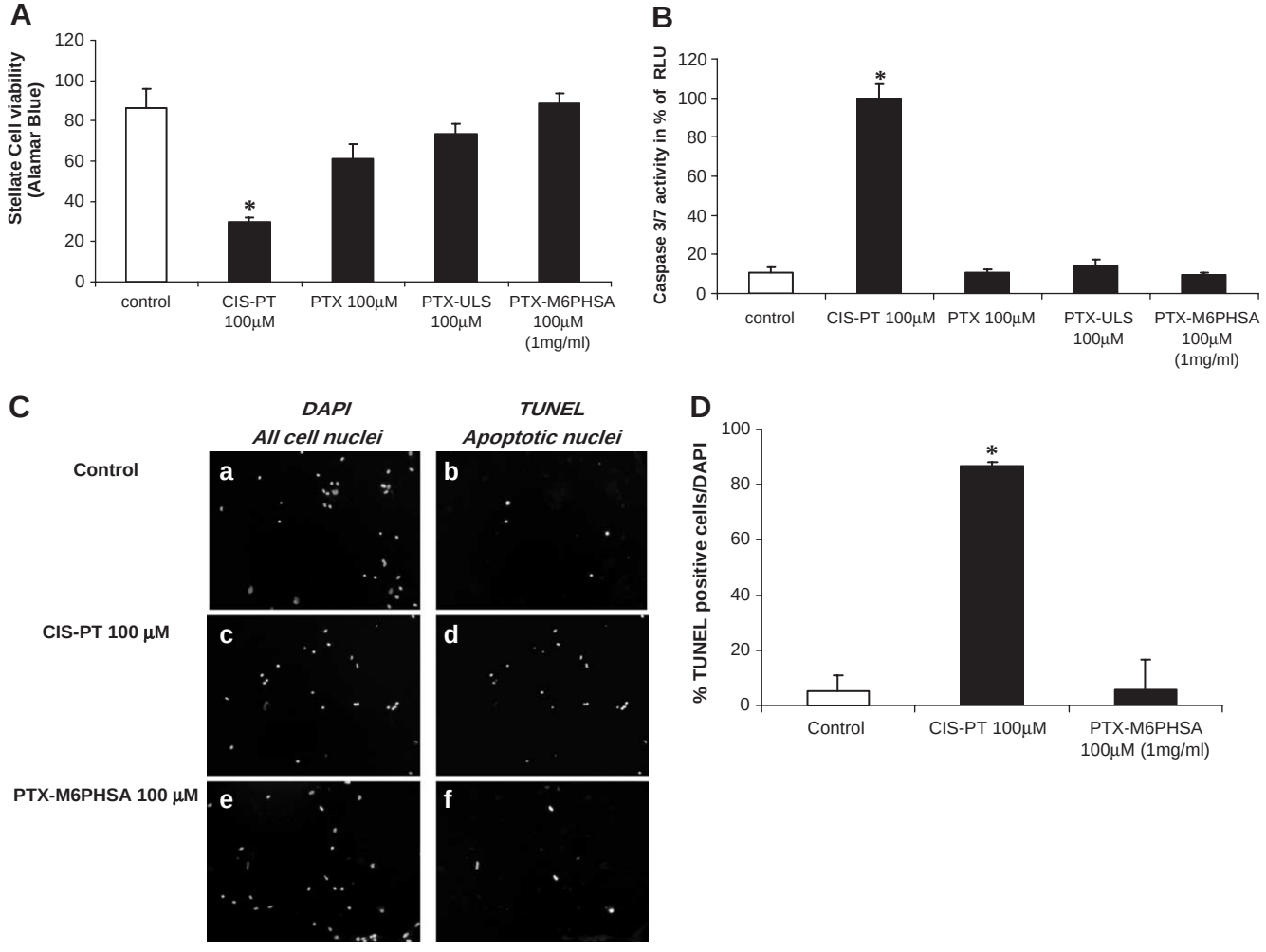

Fig. 6. Effect of PTX–M6PHSA on apoptosis. HSC were incubated for 24 h with cisplatin, PTX, PTX-ULS (100 μM) or PTX–M6PHSA at a concentration of 1 mg/ml, which is equivalent to 100 μM cisplatin. A) Alamar Blue viability assay. Fluorescence was corrected for background fluorescence of Alamar Blue reagent in medium without cells *: $p<0.05$ vs control HSC. B) Caspase 3/7 activity assay using a luminescent caspase substrate. Emitted light units were normalized relative to the signal of cisplatin treated HSC. RLU: relative light units, *: $p<0.05$ vs basal levels. C) Activated HSC, cisplatin or PTX–M6PHSA induced apoptosis as assayed by TUNEL staining. Activated Stellate cells (a, b) were incubated with 100 μM cisplatin (c, d) or PTX–M6PHSA at 100 μM (e, f). Nuclei were stained with DAPI (left column) to localize the nuclei of all cells, or TUNEL (right column) to visualize nuclei of apoptotic cells. Cisplatin treatment induced apoptosis in almost all cells, while PTX–M6PHSA treatment is comparable with control HSC. Magnification 10×. D) Quantification of TUNEL positive cells per treatment *: $p<0.05$ vs control HSC.

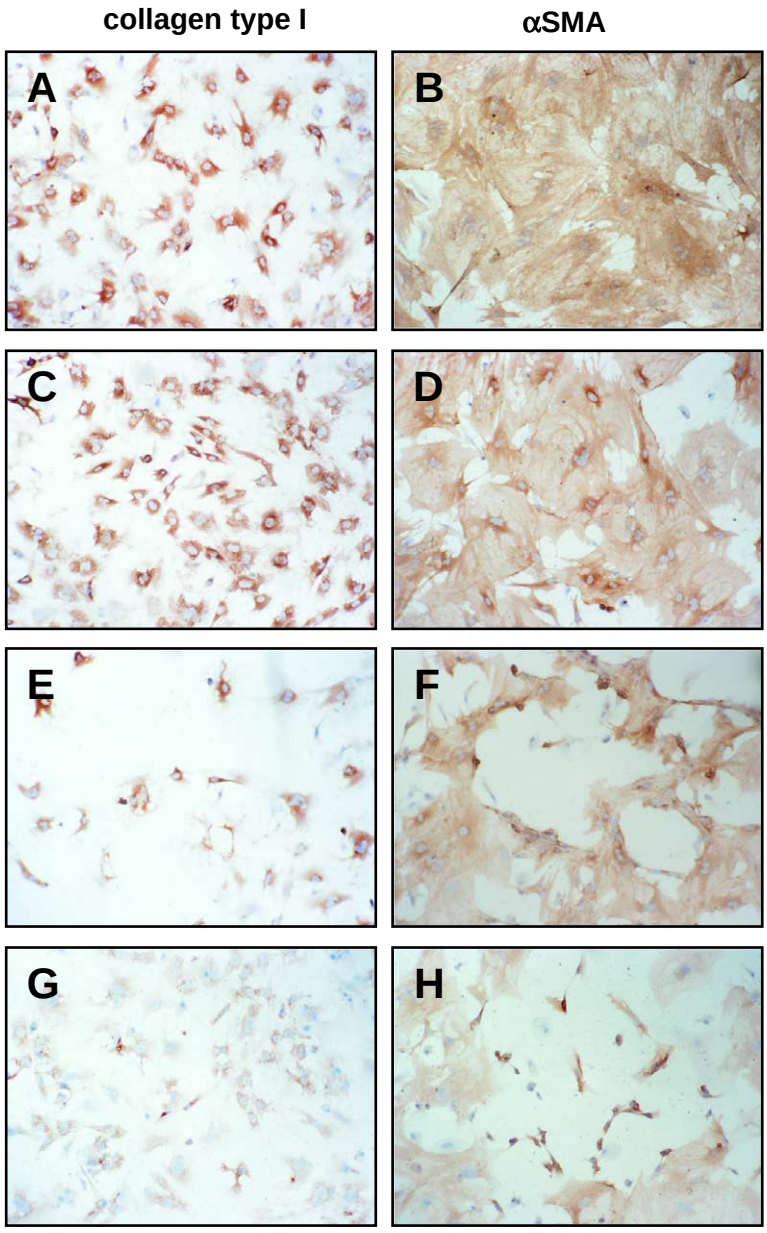

Fig. 7. Effects of PTX–M6PHSA on fibrosis markers collagen I and α-SMA. HSC were incubated for 24 h with PTX-HSA, PTX–M6PHSA (both at 1 mg/ml, equivalent to 100 μM PTX), or 1 mM non-targeted PTX. Cells were stained for collagen type I or α-SMA and counterstained with hematoxillin. A, B) Stellate cells and incubation with: C, D) PTX-HSA; E, F) PTX–M6PHSA; G, H) non-targeted PTX. Magnification 10×.

vitro antifibrotic activity. Furthermore, the novel platinum-linker afforded straightforward synthesis of conjugates that display slow-release of the coupled drug.

Over the past decades, drug delivery research has invested great efforts to find appropriate linkage systems for the preparation of drug-carrier conjugates [19,20]. Many drug candidates however lack the appropriate functional groups for commonly applied conjugation strategies. Although the presently investigated drug, PTX, also offers other options for conjugation (e.g. hydrazone linkage at its keto functional group), we believe that the ULS linker has several properties that make it a valuable technology for drug delivery. First, ULS can be applied for conjugation of drug molecules that contain aromatic nitrogens. Such groups are present in the chemical structure of many drug molecules. The ULS linker can therefore facilitate conjugation of drug molecules that cannot be coupled via existing concepts. Second, synthesis of drug-ULS adducts is straightforward and can be performed at high yields. This may enable synthesis of drug-carrier conjugates even at low quantities of the drug. An additional advantage of ULS is that sulfur atoms are reacted readily with the ULS linker [15,16]. This provided a convenient approach for coupling PTX-ULS to M6PHSA, since high drug : carrier ratios were found in the final product. Lastly, the slow drug release profile is different from existing drug–carrier conjugates. This may afford continuous drug release during a period of days, which is not possible with existing linkages.

Our in vitro stability/drug-release studies indicated that the release of PTX was driven by chemical displacement by coordinating ligands for Pt(II). Within a biological matrix, such ligands are for instance glutathione and ligands containing sulfur atoms (e.g. methionine) or aromatic nitrogens (nucleotides, histidines). Since platinum reacts fast with thiols but slower with aromatic nitrogens, we think that competitive displacement by glutathione is a very likely mechanism for drug release. At present we can only hypothesize on the fate of the conjugate after internalization. Drug release may occur in the lysosomes, the compartment to which M6PHSA is routed after internalization [6]. Another possibility is that drug release will occur in multiple steps, in which the albumin is degraded by lysosomal enzymes first, followed by competitive drug release by thiols in other intracellular compartments. Although intracellular drug release will be most likely slow, the rapid uptake of M6PHSA by target cells within the fibrotic liver (Fig. 4) will favor intracellular release of the conjugated PTX from PTX–M6PHSA.

An important concern raised in relation to the use of platinum-derivatives is their potential cisplatin-related toxicity. Many different platinum compounds have been investigated for their cell-killing properties in vitro as well as in vivo [21]. One generally accepted mechanism of cisplatin toxicity involves cross-linking of DNA, leading to cell death via apoptotic or necrotic pathways [22]. Hence, the toxicity of cisplatin and other platinum(II) compounds is closely related to the availability of reactive ligand sites at the platina atom. Since in PTX–M6PHSA the platinum is fully coordinated, it can only react with endogenous compounds after release of the drug or carrier. The platinum–ethylendiammine bridge in ULS is considered very stable. As the release of drug (or carrier) is slow, only low concentrations of reactive platinum are present in the target cells. Furthermore, cisplatin is readily detoxified by binding to low-molecular weight thiols and thiol groups in proteins, especially at lower concentrations. We expect that glutathione adducts will be the major metabolites resulting from the linker, and we will investigate this more extensively in future studies. Our present results demonstrate that both PTX-ULS and PTX–M6PHSA do not produce toxic metabolites and we conclude that novel ULS linker is safe, despite the cisplatin related structure.

PTX–M6PHSA reduced the production of collagen I notably, an effect that must be attributed to the delivery of PTX into the HSC, since no effect was observed after treatment with either PTX-HSA or FLU-M6PHSA. In addition, we observed striking changes on the morphology of the cells, which were not observed after treatment with free PTX. Although the observed changes in morphology suggest that the cells may detach and die (anoikis), we did not observe this in our apoptosis or viability assays. Moreover, the elimination of fibrogenic HSC by PTX–M6PHSA may be a beneficial effect in the treatment of liver fibrosis, apart from antifibrotic effects by reducing collagen deposition. We therefore concluded that PTX–M6PHSA is a promising candidate for further evaluation as antifibrotic therapy.

Apart from the presently investigated conjugate, PTX–M6PHSA, ULS allows coupling of many other antifibrotic drug candidates that contain aromatic nitrogen donor groups. In this respect, we have investigated the delivery of the angiotensin II antagonist losartan, which shows promising results in animal models of fibrosis and is tested clinically in cirrhotic patients [1,23]. Losartan was coupled to M6PHSA according to similar protocols as described for PTX [24]. Preliminary results indicate that daily injections with losartan-M6PHSA attenuated BDL liver fibrosis, while no toxicity was observed. Together with the presently discussed results on PTX–M6PHSA, this indicates the potential of platinum-coordination chemistry as a novel modality to prepare drug targeting preparations.

Acknowledgements

We kindly acknowledge Anne-Miek van Loenen, Jan Visser, Chantal Pottgens, Hans Pol and Jan Willem Kok for assistance in different experimental procedures. Marie Lacombe, Jan Reedijk, Elena Pantoja, and Anne Kalayda are thanked for valuable scientific discussions relating to the experiments.

Financial support for this project has been granted by SenterNovem (grant TSGE1083) and by the EU Marie Curie fellowship program (grant HPMI-CT-2002-00218).

References

[1] R. Bataller, D.A. Brenner, Liver fibrosis, J. Clin. Invest. 1152 (2005) 209–218.
[2] L. Beljaars, G. Molema, B. Weert, H. Bonnema, P. Olinga, G.M.M. Groothuis, D.K.F. Meijer, K. Poelstra, Albumin modified with mannose 6-phosphate: a potential carrier for selective delivery of antifibrotic drugs to rat and human hepatic stellate cells, Hepatology 295 (1999) 1486–1493.
[3] R. Bataller, D.A. Brenner, Hepatic stellate cells as a target for the treatment of liver fibrosis, Semin. Liver Dis. 213 (2001) 437–451.
[4] S.L. Friedman, The virtuosity of hepatic stellate cells, Gastroenterology 1175 (1999) 1244–1246.
[5] S.L. Friedman, Liver fibrosis—from bench to bedside, J. Hepatol. 38 (Suppl 1) (2003) S38–S53.
[6] L. Beljaars, P. Olinga, G. Molema, P. De Bleser, A. Geerts, G.M.M. Groothuis, D.K.F. Meijer, K. Poelstra, Characteristics of the hepatic stellate cell-selective carrier mannose 6-phosphate modified albumin ($M6P_{28}$-HSA), Liver 215 (2001) 320–328.
[7] L. Beljaars, G. Molema, D. Schuppan, A. Geerts, P.J. De Bleser, B. Weert, D.K.F. Meijer, K. Poelstra, Successful targeting of albumin to rat hepatic stellate cells using albumin modified with cyclic peptides that recognize the collagen type VI receptor, J. Biol. Chem. 27517 (2000) 12743–12751.
[8] R. Greupink, H.I. Bakker, C. Reker-Smit, A. van Loenen-Weemaes, R.J. Kok, D.K.F. Meijer, L. Beljaars, K. Poelstra, Studies on the targeted delivery of the antifibrogenic compound mycophenolic acid to the hepatic stellate cell, J. Hepatol. xx (2005) x.
[9] C. Windmeier, A.M. Gressner, Effect of pentoxifylline on the fibrogenic functions of cultured rat liver fat-storing cells and myofibroblasts, Biochem. Pharmacol. 515 (3–8) (1996) 577–584.
[10] A. Desmoulière, G. Xu, A.M.A. Costa, I.M. Yousef, G. Gabbiani, B. Tuchweber, Effect of pentoxifylline on early proliferation and phenotypic modulation of fibrogenic cells in two rat models of liver fibrosis and on cultured hepatic stellate cells, J. Hepatol. 304 (1999) 621–631.
[11] C. Raetsch, J.D. Jia, G. Boigk, M. Bauer, E.G. Hahn, E.-O. Riecken, D. Schuppan, Pentoxifylline downregulates profibrogenic cytokines and

procollagen I expression in rat secondary biliary fibrosis, Gut 502 (2002) 241–247.
[12] Y.M. Chen, K.D. Wu, T.J. Tsai, B.S. Hsieh, Pentoxifylline inhibits PDGF-induced proliferation of and TGF-beta-stimulated collagen synthesis by vascular smooth muscle cells, J. Mol. Cell. Cardiol. 314 (1999) 773–783.
[13] R.P. Gude, M.M. Binda, A.L. Boquete, R.D. Bonfil, Inhibition of endothelial cell proliferation and tumor-induced angiogenesis by pentoxifylline, J. Cancer Res. Clin. Oncol. 12710 (2001) 625–630.
[14] T. Krakauer, Pentoxifylline inhibits ICAM-1 expression and chemokine production induced by proinflammatory cytokines in human pulmonary epithelial cells, Immunopharmacology 463 (2000) 253–261.
[15] R.P. van Gijlswijk, E.G. Talman, I. Peekel, J. Bloem, M.A. van Velzen, R. J. Heetebrij, H.J. Tanke, Use of horseradish peroxidase- and fluorescein-modified cisplatin derivatives for simultaneous labeling of nucleic acids and proteins, Clin. Chem. 488 (2002) 1352–1359.
[16] R.J. Heetebrij, E.G. Talman, M.A. Velzen, R.P. van Gijlswijk, S.S. Snoeijers, M. Schalk, J. Wiegant, F. Rijke, R.M. Kerkhoven, A.K. Raap, H.J. Tanke, J. Reedijk, H.J. Houthoff, Platinum(II)-based coordination compounds as nucleic acid labeling reagents: synthesis, reactivity, and applications in hybridization assays, ChemBioChem. 47 (7–7) (2003) 573–583.
[17] A. Geerts, T. Niki, K. Hellemans, D. De Craemer, K. Van den Berg, J.-M. Lazou, G. Stange, M. Van de Winkel, P.J. De Bleser, Purification of rat hepatic stellate cells by side scatter-activated cell sorting, Hepatology 27 (1998) 590–598.
[18] Y. Gavrieli, Y. Sherman, S.A. Ben Sasson, Identification of programmed cell death in situ via specific labeling of nuclear DNA fragmentation, J. Cell Biol. 1193 (1992) 493–501.
[19] H. Soyez, E. Schacht, S. Van Der Kerken, The crucial role of spacer groups in macromolecular prodrug design, Adv. Drug Deliv. Rev. 212 (1996) 81–106.
[20] R.J. Kok, S.A. Ásgeirsdóttir, W.R. Verweij, in: G. Molema, D.K.F. Meijer (Eds.), Drug Targeting. Organ-Specific Strategies, WILEY-VCH Verlag GmbH, Weinheim, 2001, pp. 275–308.
[21] Y.P. Ho, S.C. Au-Yeung, K.K. To, Platinum-based anticancer agents: innovative design strategies and biological perspectives, Med. Res. Rev. 235 (2003) 633–655.
[22] M.A. Fuertes, J. Castilla, C. Alonso, J.M. Perez, Novel concepts in the development of platinum antitumor drugs, Curr. Med. Chem. Anti.-Canc. Agents 24 (2002) 539–551.
[23] G. Castano, P. Viudez, M. Riccitelli, S. Sookoian, A randomized study of losartan vs propranolol: effects on hepatic and systemic hemodynamics in cirrhotic patients, Ann. Hepatol. 21 (2003) 36–40.
[24] T. Gonzalo, R. Bataller, P. Sancho-Bru, C. Fontdevilla, J. Swart, L. Beljaars, V. Arroyo, K. Poelstra, P. Gines, R.J. Kok, Short-term treatment with losartan targeted to activated stellate cells reduces advanced liver fibrogenesis: a new strategy to treat liver fibrosis, Hepatology 42 (604A) (2005).